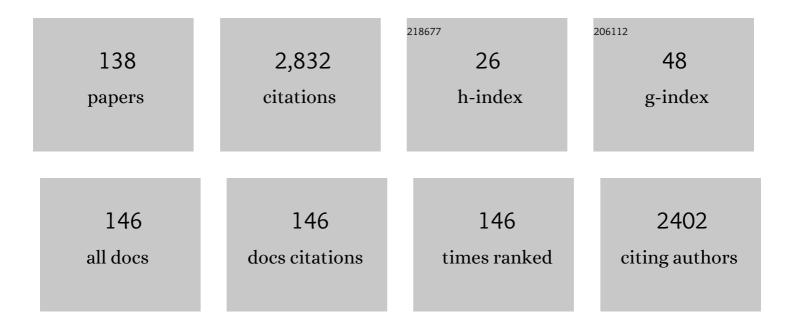
## Martin C Stennett

List of Publications by Year in descending order

Source: https://exaly.com/author-pdf/6397782/publications.pdf Version: 2024-02-01



#	Article	IF	CITATIONS
1	Immobilisation of radioactive waste in glasses, glass composite materials and ceramics. Advances in Applied Ceramics, 2006, 105, 3-12.	1.1	328
2	Effects of sintering temperature on the internal barrier layer capacitor (IBLC) structure in CaCu3Ti4O12 (CCTO) ceramics. Journal of the European Ceramic Society, 2012, 32, 3313-3323.	5.7	277
3	A Crystal-Chemical Framework for Relaxor versus Normal Ferroelectric Behavior in Tetragonal Tungsten Bronzes. Chemistry of Materials, 2015, 27, 3250-3261.	6.7	153
4	Coupling between octahedral tilting and ferroelectric order in tetragonal tungsten bronze-structured dielectrics. Applied Physics Letters, 2006, 89, 122908.	3.3	125
5	Dielectric and structural studies of Ba2MTi2Nb3O15 (BMTNO15, M=Bi3+,La3+,Nd3+,Sm3+,Gd3+) tetragonal tungsten bronze-structured ceramics. Journal of Applied Physics, 2007, 101, 104114.	2.5	110
6	An improved laboratory-based x-ray absorption fine structure and x-ray emission spectrometer for analytical applications in materials chemistry research. Review of Scientific Instruments, 2019, 90, 024106.	1.3	70
7	Nanoscale mechanism of UO2 formation through uranium reduction by magnetite. Nature Communications, 2020, 11, 4001.	12.8	57
8	Role of Microstructure and Surface Defects on the Dissolution Kinetics of CeO <sub>2</sub> , a UO <sub>2</sub> Fuel Analogue. ACS Applied Materials & Interfaces, 2016, 8, 10562-10571.	8.0	56
9	The HADES Facility for High Activity Decommissioning Engineering & Science: part of the UK National Nuclear User Facility. IOP Conference Series: Materials Science and Engineering, 2020, 818, 012022.	0.6	53
10	A new relaxor ferroelectric, Ba2LaTi2Nb3O15. Journal of Materials Chemistry, 2002, 12, 2609-2611.	6.7	45
11	A new family of ferroelectric tetragonal tungsten bronze phases, Ba2MTi2X3O15. Journal of the European Ceramic Society, 2005, 25, 2471-2475.	5.7	45
12	Temperature-dependent crystal structure of ferroelectric Ba2LaTi2Nb3O15. Journal of Materials Chemistry, 2005, 15, 798.	6.7	45
13	Effect of Zn- and Ca-oxides on the structure and chemical durability of simulant alkali borosilicate glasses for immobilisation of UK high level wastes. Journal of Nuclear Materials, 2015, 462, 321-328.	2.7	45
14	Structural Transformations and Disordering in Zirconolite (CaZrTi <sub>2</sub> O <sub>7</sub> ) at High Pressure. Inorganic Chemistry, 2013, 52, 1550-1558.	4.0	40
15	The durability of iodide sodalite. Journal of Nuclear Materials, 2014, 449, 168-172.	2.7	40
16	Preparation, characterisation and dissolution of a CeO2 analogue for UO2 nuclear fuel. Journal of Nuclear Materials, 2013, 432, 182-188.	2.7	39
17	Synthesis, structure and characterisation of the n=4 Aurivillius phase Bi5Ti3CrO15. Journal of Solid State Chemistry, 2011, 184, 252-263.	2.9	37
18	Selective behaviour of dilute Fe3+ ions in silicate glasses: an Fe K-edge EXAFS and XANES study. Journal of Non-Crystalline Solids, 2014, 387, 47-56.	3.1	36

#	Article	IF	CITATIONS
19	Proper Ferroelectricity in the Dion–Jacobson Material CsBi2Ti2NbO10: Experiment and Theory. Chemistry of Materials, 2015, 27, 8298-8309.	6.7	36
20	Impact of rare earth ion size on the phase evolution of MoO3-containing aluminoborosilicate glass-ceramics. Journal of Nuclear Materials, 2018, 510, 539-550.	2.7	35
21	Rapid synthesis of Pb5(VO4)3I, for the immobilisation of iodine radioisotopes, by microwave dielectric heating. Journal of Nuclear Materials, 2011, 414, 352-359.	2.7	32
22	Rapid low temperature synthesis of a titanate pyrochlore by molten salt mediated reaction. Journal of the European Ceramic Society, 2012, 32, 3211-3219.	5.7	30
23	Contribution of Energetically Reactive Surface Features to the Dissolution of CeO <sub>2</sub> and ThO <sub>2</sub> Analogues for Spent Nuclear Fuel Microstructures. ACS Applied Materials & Interfaces, 2014, 6, 12279-12289.	8.0	30
24	Synthesis and characterisation of Ca1-xCexZrTi2-2xCr2xO7: Analogue zirconolite wasteform for the immobilisation of stockpiled UK plutonium. Journal of the European Ceramic Society, 2020, 40, 5909-5919.	5.7	29
25	The fluorite related modulated structures of the Gd2(Zr2â^'xCex)O7 solid solution: An analogue for Pu disposition. Journal of Solid State Chemistry, 2012, 191, 2-9.	2.9	28
26	Iron phosphate glasses: Bulk properties and atomic scale structure. Journal of Nuclear Materials, 2017, 494, 342-353.	2.7	28
27	Reactive spark plasma synthesis of CaZrTi2O7 zirconolite ceramics for plutonium disposition. Journal of Nuclear Materials, 2018, 500, 11-14.	2.7	27
28	Dielectric spectra of a new relaxor ferroelectric system Ba2LnTi2Nb3O15 (Ln=La, Nd). Journal of the European Ceramic Society, 2005, 25, 3069-3073.	5.7	26
29	The Use of Surrogates in Waste Immobilization Studies: A Case Study of Plutonium. Materials Research Society Symposia Proceedings, 2008, 1107, 1.	0.1	26
30	Microanalytical X-ray Imaging of Depleted Uranium Speciation in Environmentally Aged Munitions Residues. Environmental Science & Technology, 2014, 48, 1467-1474.	10.0	26
31	Evolution of phase assemblage of blended magnesium potassium phosphate cement binders at 200° and 1000°C. Advances in Applied Ceramics, 2015, 114, 386-392.	1.1	26
32	A systematic investigation of the phase assemblage and microstructure of the zirconolite CaZr1-xCexTi2O7 system. Journal of Nuclear Materials, 2020, 535, 152137.	2.7	26
33	Crystal structure and non-stoichiometry of cerium brannerite: Ce0.975Ti2O5.95. Journal of Solid State Chemistry, 2012, 192, 172-178.	2.9	25
34	Review of zirconolite crystal chemistry and aqueous durability. Advances in Applied Ceramics, 2021, 120, 69-83.	1.1	25
35	Temperature transformation of blended magnesium potassium phosphate cement binders. Cement and Concrete Research, 2021, 141, 106332.	11.0	25
36	Remediation of soils contaminated with particulate depleted uranium by multi stage chemical extraction. Journal of Hazardous Materials, 2013, 263, 382-390.	12.4	24

#	Article	IF	CITATIONS
37	Alteration layer formation of Ca- and Zn-oxide bearing alkali borosilicate glasses for immobilisation of UK high level waste: A vapour hydration study. Journal of Nuclear Materials, 2016, 479, 639-646.	2.7	24
38	High-Pressure and -Temperature Ion Exchange of Aluminosilicate and Gallosilicate Natrolite. Journal of the American Chemical Society, 2011, 133, 13883-13885.	13.7	23
39	The Structural Role of <scp>Zn</scp> in Nuclear Waste Glasses. International Journal of Applied Glass Science, 2011, 2, 343-353.	2.0	23
40	The structure of ion beam amorphised zirconolite studied by grazing angle X-ray absorption spectroscopy. Nuclear Instruments & Methods in Physics Research B, 2010, 268, 1847-1852.	1.4	21
41	Synthesis and characterisation of Pu-doped zirconolites –(Ca <sub>1â^x</sub> Pu <sub>x</sub> )Zr(Ti <sub>2-2x</sub> Fe <sub>2x</sub> )O <sub>7</sub> . IOP Conference Series: Materials Science and Engineering, 2010, 9, 012007.	0.6	19
42	The effect of uranium oxide additions on the structure of alkali borosilicate glasses. Journal of Non-Crystalline Solids, 2013, 378, 282-289.	3.1	19
43	Multi-scale investigation of uranium attenuation by arsenic at an abandoned uranium mine, South Terras. Npj Materials Degradation, 2017, 1, .	5.8	19
44	Characterisation and disposability assessment of multi-waste stream in-container vitrified products for higher activity radioactive waste. Journal of Hazardous Materials, 2021, 401, 123764.	12.4	19
45	Insights into the fabrication and structure of plutonium pyrochlores. Journal of Materials Chemistry A, 2020, 8, 2387-2403.	10.3	17
46	Krypton irradiation damage in Nd-doped zirconolite and perovskite. Journal of Nuclear Materials, 2011, 415, 67-73.	2.7	16
47	A preliminary validation study of PuO2 incorporation into zirconolite glass-ceramics. MRS Advances, 2018, 3, 1065-1071.	0.9	16
48	Tungsten Bronze-Structured Temperature-Stable Dielectrics. Journal of the American Ceramic Society, 2007, 90, 980-982.	3.8	15
49	Thermal treatment of simulant plutonium contaminated materials from the Sellafield site by vitrification in a blast-furnace slag. Journal of Nuclear Materials, 2014, 444, 186-199.	2.7	15
50	The effect of pre-treatment parameters on the quality of glass-ceramic wasteforms for plutonium immobilisation, consolidated by hot isostatic pressing. Journal of Nuclear Materials, 2017, 485, 253-261.	2.7	15
51	Combined Quantitative X-ray Diffraction, Scanning Electron Microscopy, and Transmission Electron Microscopy Investigations of Crystal Evolution in CaO–Al <sub>2</sub> 0 <sub>3</sub> –SiO <sub>2</sub> –TiO <sub>2</sub> –TiO <sub>2</sub> –ZrO <sub>2</sub> –Nd System, Crystal Growth and Design, 2017, 17, 1079-1087.	<sub>2<td>ub<sup>15</sup>O<sub>3</sub></td></sub>	ub <sup>15</sup> O <sub>3</sub>
52	Synthesis and characterisation of brannerite compositions (U0.9Ce0.1)1â^'xMxTi2O6 (M = Gd3+, Ca2+) for the immobilisation of MOX residues. RSC Advances, 2018, 8, 2092-2099.	3.6	15
53	Tuning between Proper and Hybrid-Improper Mechanisms for Polar Behavior in CsLn2Ti2NbO10 Dion-Jacobson Phases. Chemistry of Materials, 2020, 32, 8700-8712.	6.7	14
54	Krypton and helium irradiation damage in neodymium–zirconolite. Journal of Nuclear Materials, 2011, 416, 221-224.	2.7	13

#	Article	IF	CITATIONS
55	The thermal decomposition of studtite: analysis of the amorphous phase. Journal of Radioanalytical and Nuclear Chemistry, 2021, 327, 1335-1347.	1.5	13
56	Synthesis, characterisation and corrosion behaviour of simulant Chernobyl nuclear meltdown materials. Npj Materials Degradation, 2020, 4, .	5.8	13
57	Sintering of CaF2 pellets as nuclear fuel analog for surface stability experiments. Journal of Nuclear Materials, 2011, 419, 46-51.	2.7	12
58	Solution composition and particle size effects on the dissolution and solubility of a ThO2 microstructural analogue for UO2 matrix of nuclear fuel. Radiochimica Acta, 2015, 103, 565-576.	1.2	12
59	Simulation of alpha decay of actinides in iron phosphate glasses by ion irradiation. Nuclear Instruments & Methods in Physics Research B, 2016, 371, 424-428.	1.4	12
60	Synthesis, structure, and characterization of the thorium zirconolite CaZr <sub>1â€x</sub> Th <sub>x</sub> Ti <sub>2</sub> O <sub>7</sub> system. Journal of the American Ceramic Society, 2021, 104, 2937-2951.	3.8	12
61	Phase Evolution in the CaZrTi <sub>2</sub> O <sub>7</sub> –Dy <sub>2</sub> Ti <sub>2</sub> O <sub>7</sub> System: A Potential Host Phase for Minor Actinide Immobilization. Inorganic Chemistry, 2022, 61, 5744-5756.	4.0	12
62	X-ray diffraction data for the new ferroelectric tetragonal tungsten bronze phases, Ba2RETi2M3O15:M=Nb and RE=La, Pr, Nd, Sm, Gd, Dy, (Bi);M=Ta and RE=La, Nd. Powder Diffraction, 2005, 20, 43-46.	0.2	11
63	Investigation of Ce incorporation in zirconolite glass-ceramics for UK plutonium disposition. MRS Advances, 2017, 2, 699-704.	0.9	11
64	Nonresonant valence-to-core x-ray emission spectroscopy of niobium. Physical Review B, 2018, 97, .	3.2	11
65	Influence of Lubricants and Attrition Milling Parameters on the Quality of Zirconolite Ceramics, Consolidated by Hot Isostatic Pressing, for Immobilization of Plutonium. International Journal of Applied Ceramic Technology, 2015, 12, E92.	2.1	10
66	Immobilisation of Prototype Fast Reactor raffinate in a barium borosilicate glass matrix. Journal of Nuclear Materials, 2018, 508, 203-211.	2.7	10
67	Effect of Ti4+ on the structure of nepheline (NaAlSiO4) glass. Geochimica Et Cosmochimica Acta, 2020, 290, 333-351.	3.9	10
68	Structure of NaFeSiO4, NaFeSi2O6, and NaFeSi3O8 glasses and glass-ceramics. American Mineralogist, 2020, 105, 1375-1384.	1.9	10
69	Encapsulation of TRISO particle fuel in durable soda-lime-silicate glasses. Journal of Nuclear Materials, 2013, 436, 139-149.	2.7	9
70	A new approach to the immobilisation of technetium and transuranics: Co-disposal in a zirconolite ceramic matrix. Journal of Nuclear Materials, 2020, 528, 151885.	2.7	9
71	A Feasibility Investigation of Laboratory Based X-ray Absorption Spectroscopy in Support of Nuclear Waste Management. MRS Advances, 2020, 5, 27-35.	0.9	9
72	Synthesis and Characterization of Brannerite Compositions for MOX Residue Disposal. MRS Advances, 2017, 2, 557-562.	0.9	8

#	Article	IF	CITATIONS
73	Synthesis and characterisation of the hollandite solid solution Ba1.2-xCsxFe2.4-xTi5.6+xO16 for partitioning and conditioning of radiocaesium. Journal of Nuclear Materials, 2018, 503, 164-170.	2.7	8
74	The formation of stoichiometric uranium brannerite (UTi2O6) glass-ceramic composites from the component oxides in a one-pot synthesis. Journal of Nuclear Materials, 2020, 542, 152516.	2.7	8
75	Safely probing the chemistry of Chernobyl nuclear fuel using micro-focus X-ray analysis. Journal of Materials Chemistry A, 2021, 9, 12612-12622.	10.3	8
76	Influence of accessory phases and surrogate type on accelerated leaching of zirconolite wasteforms. Npj Materials Degradation, 2021, 5, .	5.8	8
77	Symmetry and the Role of the Anion Sublattice in Aurivillius Oxyfluoride Bi2TiO4F2. Inorganic Chemistry, 2021, 60, 14105-14115.	4.0	8
78	Synthesis of Ca1-xCexZrTi2-2xAl2xO7 zirconolite ceramics for plutonium disposition. Journal of Nuclear Materials, 2021, 556, 153198.	2.7	8
79	Synthesis and characterisation of Ce-doped zirconolite Ca0.80Ce0.20ZrTi1.60M0.40O7 (M = Fe, Al) formed by reactive spark plasma sintering (RSPS). MRS Advances, 2022, 7, 75-80.	0.9	8
80	Transformation of Cs-IONSIV® into a ceramic wasteform by hot isostatic pressing. Journal of Nuclear Materials, 2018, 498, 33-43.	2.7	7
81	The Effect of A-Site Cation on the Formation of Brannerite (ATi2O6, A = U, Th, Ce) Ceramic Phases in a Glass-Ceramic Composite System. MRS Advances, 2020, 5, 73-81.	0.9	7
82	Synthesis, Characterization, and Crystal Structure of Dominant Uranium(V) Brannerites in the UTi <sub>2–<i>x</i></sub> Al <sub><i>x</i></sub> O <sub>6</sub> System. Inorganic Chemistry, 2021, 60, 18112-18121.	4.0	7
83	Solubility, speciation and local environment of chlorine in zirconolite glass–ceramics for the immobilisation of plutonium residues. RSC Advances, 2020, 10, 32497-32510.	3.6	6
84	Mössbauer studies of materials used to immobilise industrial wastes. Hyperfine Interactions, 2013, 217, 83-90.	0.5	5
85	Graphite immobilisation in iron phosphate glass composite materials produced by microwave and conventional sintering routes. Journal of Nuclear Materials, 2014, 454, 343-351.	2.7	5
86	Solution Composition Effects on the Dissolution of a CeO2 analogue for UO2 and ThO2 nuclear fuels. Materials Research Society Symposia Proceedings, 2015, 1744, 185-190.	0.1	5
87	Synthesis of simulant â€~lava-like' fuel containing materials (LFCM) from the Chernobyl reactor Unit 4 meltdown. MRS Advances, 2017, 2, 609-614.	0.9	5
88	Radiation stability study on cerium loaded iron phosphate glasses by ion irradiation method. Journal of Radioanalytical and Nuclear Chemistry, 2020, 323, 1381-1386.	1.5	5
89	Thermal treatment of nuclear fuel-containing Magnox sludge radioactive waste. Journal of Nuclear Materials, 2021, 552, 152965.	2.7	5
90	The Effect of Temperature on the Stability and Cerium Oxidation State of CeTi2O6 in Inert and Oxidizing Atmospheres. Inorganic Chemistry, 2020, 59, 17364-17373.	4.0	5

#	Article	IF	CITATIONS
91	Spectroscopic evaluation of U <sup>VI</sup> –cement mineral interactions: ettringite and hydrotalcite. Journal of Synchrotron Radiation, 2022, 29, 89-102.	2.4	5
92	Microchemical and crystallographic characterisation of fluorite-based ceramic wasteforms. Materials Research Society Symposia Proceedings, 2006, 932, 1.	0.1	4
93	Rapid microwave synthesis of Pb5(VO4)3X (X = F, Cl, Br and I) vanadinite apatites for the immobilisation of halide radioisotopes Materials Research Society Symposia Proceedings, 2012, 1475, 221.	0.1	4
94	Thermal Conversion of Cs-exchanged IONSIV IE-911 into a Novel Caesium Ceramic Wasteform by Hot Isostatic Pressing. Materials Research Society Symposia Proceedings, 2013, 1518, 67-72.	0.1	4
95	Molten salt synthesis of Ce doped zirconolite for the immobilisation of pyroprocessing wastes and separated plutonium. Ceramics International, 2020, 46, 29080-29089.	4.8	4
96	Synthesis and characterization of iodovanadinite using PdI <sub>2,</sub> an iodine source for the immobilisation of radioiodine. RSC Advances, 2020, 10, 25116-25124.	3.6	4
97	Synthesis and characterisation of transition metal substituted barium hollandite ceramics. Materials Research Society Symposia Proceedings, 2006, 932, 1.	0.1	3
98	Towards a Single Host Phase Ceramic Formulation for UK Plutonium Disposition. Materials Research Society Symposia Proceedings, 2008, 1107, 1.	0.1	3
99	Piezoelectric and ferroelectric properties of new Pb9Ce2Ti12O36 and lead-free Ba2NdTi2Nb3O15 ceramics. Journal of Electroceramics, 2010, 25, 116-121.	2.0	3
100	Decontamination of Molten Salt Wastes for Pyrochemical Reprocessing of Nuclear Fuels. Materials Research Society Symposia Proceedings, 2013, 1518, 97-102.	0.1	3
101	Silicon oxycarbide glass for the immobilisation of irradiated graphite waste. Journal of Nuclear Materials, 2016, 469, 51-56.	2.7	3
102	On the existence of AgM <sub>9</sub> (VO <sub>4</sub> ) <sub>6</sub> I (M = Ba, Pb). RSC Advances, 2017, 7, 49004-49009.	3.6	3
103	Synthesis and characterisation of high ceramic fraction brannerite (UTi2O6) glass-ceramic composites. IOP Conference Series: Materials Science and Engineering, 2020, 818, 012018.	0.6	3
104	Influence of Transition Metal Charge Compensation Species on Phase Assemblage in Zirconolite Ceramics for Pu Immobilisation. MRS Advances, 2020, 5, 93-101.	0.9	3
105	Multimodal X-ray microanalysis of a UFeO <sub>4</sub> : evidence for the environmental stability of ternary U( <scp>v</scp> ) oxides from depleted uranium munitions testing. Environmental Sciences: Processes and Impacts, 2020, 22, 1577-1585.	3.5	3
106	Synthesis and characterisation of HIP Ca0.80Ce0.20ZrTi1.60Cr0.40O7 zirconolite and observations of the ceramic–canister interface. MRS Advances, 2021, 6, 112-118.	0.9	3
107	Low-Temperature Nitridation of Fe <sub>3</sub> O <sub>4</sub> by Reaction with NaNH <sub>2</sub> . Inorganic Chemistry, 2021, 60, 2553-2562.	4.0	3
108	Chemical structure and dissolution behaviour of CaO and ZnO containing alkali-borosilicate glass. Materials Advances, 2022, 3, 1747-1758.	5.4	3

#	Article	IF	CITATIONS
109	Chemical characterisation of degraded nuclear fuel analogues simulating the Fukushima Daiichi nuclear accident. Npj Materials Degradation, 2022, 6, .	5.8	3
110	Characterisation of Plasma Vitrified Simulant Plutonium Contaminated Material Waste. Materials Research Society Symposia Proceedings, 2006, 985, 1.	0.1	2
111	The Relative Merits of Oxides of Hafnium, Cerium and Thorium as Surrogates for Plutonium Oxide in Calcium Phosphate Ceramics. Materials Research Society Symposia Proceedings, 2009, 1193, .	0.1	2
112	Ceramic Immobilisation Options for Technetium. Materials Research Society Symposia Proceedings, 2012, 1518, 111-116.	0.1	2
113	Surface Sensitive Spectroscopy Study of Ion Beam Irradiation Induced Structural Modifications in Borosilicate Glasses. Materials Research Society Symposia Proceedings, 2013, 1514, 75-80.	0.1	2
114	Investigation of Processing Parameters for the Consolidation of Actinide Glass-Ceramic Wasteforms by Hot Isostatic Pressing. MRS Advances, 2016, 1, 4269-4274.	0.9	2
115	Ceramic Immobilization Options for Technetium. MRS Advances, 2017, 2, 753-758.	0.9	2
116	Synthesis, characterisation and preliminary corrosion behaviour assessment of simulant Fukushima nuclear accident fuel debris. MRS Advances, 2020, 5, 65-72.	0.9	2
117	Ba1.2-xCsxM1.2-x/2Ti6.8+x/2O16 (M = Ni, Zn) hollandites for the immobilisation of radiocaesium. MRS Advances, 2020, 5, 55-64.	0.9	2
118	Nuclear forensic signatures and structural analysis of uranyl oxalate, its products of thermal decomposition and Fe impurity dopant. Journal of Radioanalytical and Nuclear Chemistry, 2021, 327, 957-973.	1.5	2
119	A preliminary investigation of the molten salt mediated synthesis of Gd2TiO5 â€ <sup>-</sup> stuffed' pyrochlore. MRS Advances, 2021, 6, 149-153.	0.9	2
120	In Situ Characterisation of Model UK Nuclear Waste Glasses by X-ray Absorption Spectroscopy Under Process Conditions. Materials Research Society Symposia Proceedings, 2008, 1107, 1.	0.1	1
121	The Use of High Durability Alumino-Borosilicate Glass for the Encapsulation of High Temperature Reactor (HTR) Fuel. Materials Research Society Symposia Proceedings, 2013, 1518, 3-8.	0.1	1
122	Reducing the uncertainty of nuclear fuel dissolution: an investigation of UO2 analogue CeO2. Materials Research Society Symposia Proceedings, 2013, 1518, 151-156.	0.1	1
123	Ion Beam Irradiation Induced Structural Modifications in Iron Phosphate Glasses: A Model System for Understanding Radiation Damage in Nuclear Waste Glasses. Materials Research Society Symposia Proceedings, 2015, 1757, 65.	0.1	1
124	Thermal treatment of plutonium contaminated material (PCM) waste. MRS Advances, 2017, 2, 735-740.	0.9	1
125	A synchrotron X-ray spectroscopy study of titanium co-ordination in explosive melt glass derived from the trinity nuclear test. RSC Advances, 2019, 9, 12921-12927.	3.6	1
126	Preliminary investigation of chlorine speciation in zirconolite glass-ceramics for plutonium residues by analysis of Cl K-edge XANES. MRS Advances, 2020, 5, 37-43.	0.9	1

#	Article	IF	CITATIONS
127	Laboratory Based X-ray Absorption Spectroscopy of Iron Phosphate Glasses for Radioactive Waste Immobilisation: A Preliminary Investigation IOP Conference Series: Materials Science and Engineering, 2020, 818, 012020.	0.6	1
128	Hot Isostatic Pressing (HIP): A novel method to prepare Cr-doped UO2 nuclear fuel. MRS Advances, 2020, 5, 45-53.	0.9	1
129	Ce and U speciation in wasteforms for thermal treatment of plutonium bearing wastes, probed by L3 edge XANES. IOP Conference Series: Materials Science and Engineering, 2020, 818, 012019.	0.6	1
130	An Evaluation of Single Phase Ceramic Formulations for Plutonium Disposition. Materials Research Society Symposia Proceedings, 2006, 985, 1.	0.1	0
131	Synthesis of Crystalline Ceramics for Actinide Immobilisation. , 2007, , 255.		0
132	Octahedral Tilting and Ferroelectric Order in Tetragonal Tungsten Bronze-Like Dielectrics. Applications of Ferroelectrics, IEEE International Symposium on, 2007, , .	0.0	0
133	Heavy ion implantation combined with grazing incidence X-ray absorption spectroscopy (GIXAS): A new methodology for the characterisation of radiation damage in nuclear ceramics. Materials Research Society Symposia Proceedings, 2009, 1193, .	0.1	0
134	Stability of Cs-Ionsiv in Portland cement blends for radioactive waste disposal. Materials Research Society Symposia Proceedings, 2010, 1265, 1.	0.1	0
135	Krypton and Helium Irradiation Damage in Yttria-stabilised Zirconia. Materials Research Society Symposia Proceedings, 2011, 1298, 197.	0.1	0
136	Advanced Gas-cooled Reactor SIMFuel Fabricated by Hot Isostatic Pressing: a Feasibility Investigation. IOP Conference Series: Materials Science and Engineering, 2020, 818, 012011.	0.6	0
137	Use of WetSEM® capsules for convenient multimodal scanning electron microscopy, energy dispersive X-ray analysis, and micro Raman spectroscopy characterisation of technetium oxides. Journal of Radioanalytical and Nuclear Chemistry, 2021, 328, 1313-1318.	1.5	0
138	<i>HERMES</i> – a GUI-based software tool for pre-processing of X-ray absorption spectroscopy data from laboratory Rowland circle spectrometers. Journal of Synchrotron Radiation, 2022, 29, 276-279.	2.4	0